OXFORD

SOT | Society of Toxicology
www.toxsci.oxfordjournals.org

TOXICOLOGICAL SCIENCES, 144(1), 2015, 105–113

doi: 10.1093/toxsci/kfu259
Advance Access Publication Date: December 8, 2014

Functional and Molecular Effects of Mercury Compounds on the Human OCTN1 Cation Transporter: C50 and C136 Are the Targets for Potent Inhibition

Michele Galluccio[1], Lorena Pochini[1], Valentina Peta, Maria Iannì, Mariafrancesca Scalise, and Cesare Indiveri[2]

Department DiBEST (Biologia, Ecologia, Scienze della Terra) Unit of Biochemistry and Molecular Biotechnology, Via Bucci 4C, University of Calabria, 87036 Arcavacata di Rende, Italy

[1]These authors contributed equally to this study.
[2]To whom correspondence should be addressed. Fax +39 0984-492986. E-mail: cesare.indiveri@unical.it.

ABSTRACT

The effect of mercury compounds has been tested on the organic cation transporter, hOCTN1. $MeHg^{+}$, Hg^{2+}, or Cd^{2+} caused strong inhibition of transport. 1,4-Dithioerythritol (DTE), cysteine (Cys), and N-acetyl-L-cysteine reversed (NAC) the inhibition at different extents. 2-Aminoethyl methanethiosulfonate hydrobromide (MTSEA), a prototype SH reagent, exerted inhibition of transport similar to that observed for the mercurial agents. To investigate the mechanism of action of mercurials, mutants of hOCTN1 in which each of the Cys residues was substituted by Ala have been constructed, over-expressed in *Escherichia coli*, and purified. Tetraethylammonium chloride (TEA) uptake mediated by each mutant in proteoliposomes was comparable to that of wild type (WT). IC_{50} values of the WT and mutants for the mercury compounds were derived from dose-response analyses. The mutants C50A and C136A showed significant increase of IC_{50} indicating that the 2 Cys residues were involved in the interaction with the mercury compounds and inhibition of the transporter. The double mutant C50A/C136A was constructed; the lack of inhibition confirmed that the 2 Cys residues are the targets of mercury compounds. MTSEA showed similar behavior with respect to the mercurial reagents with the difference that increased IC_{50} was observed also in the C81A mutant. Similar results were obtained when transport was measured as acetylcholine uptake. Ethyl mercury (Thimerosal) inhibited hOCTN1 as well. C50A, C50A/C136A and, at very lower extent, C136A showed increased IC_{50} indicating that C50 was the major target of this mercury compound. The homology model of hOCTN1 was built using as template PiPT and validated by the experimental data on mutant proteins.

Key words: liposomes; methylmercury; ethylmercury; toxicology; mutagenesis; acetylcholine

Organic cation transporter, OCTN1 is a member of the "Organic Cation Transporters Novel" sub-family (Tamai *et al.*, 2000) which originated in vertebrates (Eraly *et al.*, 2004). Differently from the other 2 members of the sub-family, OCTN1 shows low transport capacity for carnitine (Indiveri *et al.*, 2010; Lamhonwah and Tein, 2006; Pochini *et al.*, 2011; Scalise *et al.*, 2012). The prototype organic cation TEA has been firstly identified as substrate in cell systems over-expressing OCTN1 (Grundemann *et al.*, 2005; Lamhonwah and Tein, 2006; Nakamura *et al.*, 2008; Yabuuchi *et al.*, 1999). Ergothioneine, a fungi metabolite, was also reported to be a substrate (Grundemann *et al.*, 2005). However, the OCTN1 knockout mouse did not show any phenotype related to ergothioneine transport defect (Kato *et al.*, 2010). Using proteoliposomes reconstituted with the human OCTN1 over-expressed in bacteria, it has been shown that TEA is transported more efficiently than ergothioneine and carnitine (Pochini *et al.*, 2011). Then, this experimental system allowed the identification of acetylcholine as a transported substrate. Interestingly, reconstituted hOCTN1 has the capacity to both take up and export acetylcholine from proteoliposomes (Pochini *et al.*, 2012a,

2012b). According to these data, a physiological role of OCTN1 will lie in exporting acetylcholine from cells, acting as the missing player of the non-neuronal cholinergic system (Wessler and Kirkpatrick, 2008). This system is active in many tissues, such as airways, intestine, skin, placenta, heart, skeletal muscle, urogenital tract, and others where choline acetyltransferase, acetylcholine receptors, and cholinesterase are expressed. In these districts, acetylcholine, exported from cells, controls several cell functions with autocrine and paracrine effects (Wessler and Kirkpatrick, 2008). Acetylcholine delivered by OCTN1 interacts with α-7 nicotinic receptors regulating inflammatory responses by inhibiting release of proinflammatory mediators such as TNF-α and/or IL1-β from immune cells as part of the so-called cholinergic anti-inflammatory pathway (Rana *et al.*, 2010; Wang *et al.*, 2003; Wessler and Kirkpatrick, 2008). Therefore, hOCTN1 defects are expected to generate pathological states related with inflammation. Interestingly, the L503F-hOCTN1 variant has been associated with the Inflammatory Bowel Disease, Crohn's disease (Peltekova *et al.*, 2004; Toh *et al.*, 2013). This variant has a lower capacity to mediate acetylcholine efflux confirming a relationship with disease (Pochini *et al.*, 2012b). Moreover, the epithelial localization of OCTN1 suggests its involvement also in interactions with drugs and xenobiotics, recently demonstrated in fish where OCTN1 is involved in mercury toxicity (Yamashita *et al.*, 2013). Mercury is a harmful pollutant, present in the environment, as inorganic (Hg^{2+}) and organic form ($MeHg^{+}$) (Bridges and Zalups, 2010); it is well established that mercury exerts its toxicological action through reaction with thiol groups (van Iwaarden *et al.*, 1992). Controversial studies have been conducted also on $EthylHg^{+}$ which has been widely used as preservative in vaccines, in the form of Thimerosal from which $EthylHg^{+}$ is released and whose toxicity is still underneath (Dorea *et al.*, 2013). Molecular mechanism underlying inhibitory phenomena of mercury and its derivatives has been described for different membrane transporters (Indiveri *et al.*, 1992; Oppedisano *et al.*, 2010, 2011; Pochini *et al.*, 2013; Scalise *et al.*, 2013; Tonazzi and Indiveri, 2011). In one of these studies, effects of mercurial agents have been evaluated on rat OCTN2, demonstrating the involvement of Cys residues (Pochini *et al.*, 2013a). However, the protein extracted from animal tissues was not suitable to identify the specific residue(s) involved in responsiveness to mercury. Thus, over-expression of the recombinant hOCTN1 transporter represented an important achievement for structure/function relationship studies, given the possibility of generating specific mutants. Noteworthy, hOCTN1 harbors in its primary structure 7 Cys residues which could react with mercury compounds (Pochini *et al.*, 2011). Site-directed mutagenesis was performed in the present work to gain further insights into the molecular mechanism of interaction. Moreover, since no structures are available for animal secondary active transporters besides GLUT1 (Deng *et al.*, 2014), only homology models exist for hOCTN1. A first model constructed on the basis of the structure of the glycerol-3-phospate transporter of *Escherichia coli* (PDB 1PW4) (Hopf *et al.*, 2012; Huang *et al.*, 2003; Toh *et al.*, 2013) revealed unsuitable for topological studies since it lacks N-terminal 142 amino acid residues, containing the first transmembrane α-helix and the large extracellular loop harboring 4 Cys residues. An improved homology structural model of hOCTN1 was produced in this work, using as template the phosphate transporter (PiPT, PDB 4J05) from the eukaryotic fungus *Piriformospora indica* whose structure has been recently solved (Pedersen *et al.*, 2013). The site-directed mutagenesis combined with the novel homology modeling allowed the identification and the localization of the Cys residues responsible for the inhibition by mercury compounds. The potential links of these results with human health are discussed.

MATERIALS AND METHODS

Chemicals. Amberlite XAD-4, egg yolk phospholipids (3-sn-phosphatidylcoline from egg yolk), Sephadex G-75, TEA, acetylcholine chloride, mercury chloride (Hg^{2+}), methylmercury chloride ($MeHg^{+}$), cadmium chloride (Cd^{2+}), Thimerosal ($EtHg^{+}$), and Triton X-100 were from Sigma; acetylcholine iodide [acetyl-^{3}H]Acetylcholine and [ethyl-1-^{14}C]TEA from Perkin-Elmer; 2-aminoethyl methanethiosulfonate hydrobromide (MTSEA) from Biotium. All the other reagents were of analytical grade.

Cloning and over-expression of the Cys-Ala mutants of hOCTN1. The 7 Cys residues of OCTN1 wild type (WT) cloned in pH6EX3 vector as described in Galluccio *et al.* (2009) have been mutated to Ala by PCR overlap extension method (Ho *et al.*, 1989) using the primers reported in Supplementary Information (Supplementary Table 1). The over-expression of WT and mutant proteins has been performed, in *E. coli* Rosetta(DE3)pLysS as previously described (Galluccio *et al.*, 2009; Indiveri *et al.*, 2013).

Reconstitution of WT and mutants hOCTN1 transporters into liposomes. hOCTN1WT and Cys mutants were purified as previously described (Pochini *et al.*, 2012b). The proteins were reconstituted by removing the detergent from mixed micelles containing detergent, protein, and phospholipids by incubation with Amberlite XAD-4 in a batch-wise procedure (Pochini *et al.*, 2011). The composition of the initial mixture used for reconstitution (except when differently indicated) was 200 μl of the purified protein (6 μg protein in 0.1% Triton X-100), 120 μl of 10% Triton X-100, 120 μl of 10% egg yolk phospholipids in the form of sonicated liposomes prepared as previously described (Indiveri *et al.*, 1994), 16mM ATP di-sodium salt buffered at pH 8.0, and 10mM Tris/HCl (pH 8.5) in a final volume of 700 μl. After vortexing, this mixture was incubated with 0.50 g Amberlite XAD-4 under rotatory stirring (1200 rpm) at room temperature for 45 min.

Transport measurements. hOCTN1 was inserted in the formed proteoliposomes with the same orientation as in the cell membrane (Pochini *et al.*, 2011). Proteoliposomes (550 μl) were passed through a Sephadex G-75 column (0.7 cm diameter × 15 cm height) pre-equilibrated with 10mM Tris/HCl (pH 8.5). Proteoliposomes (550 μl) were collected from these columns and divided in aliquots (samples) of 100 μl. Transport was started by adding 0.1mM of [^{14}C]TEA or [^{3}H]Acetylcholine to the proteoliposome samples, and stopped by adding 3mM pyridoxal 5-phosphate (PLP) at the desired time interval. In control samples the inhibitor was added at time zero according to the inhibitor stop method (Palmieri and Klingenberg, 1979). The assay temperature was 25°C. Overlapping results were obtained at higher temperatures up to 37°C. In particular effects of inhibitors and IC_{50} values did not change by increasing the temperature (not shown), as it was also found for the B0AT1 (SLC6A19) transporter (Pochini *et al.*, 2014). Finally, each sample of proteoliposomes (100 μl) was passed through a Sephadex G-75 column (0.6 cm diameter × 8 cm height) in order to separate the external from the internal radioactivity. Liposomes were eluted with 1 ml of 50mM NaCl and collected in 4 ml of scintillation mixture, vortexed, and counted. The experimental values were corrected by subtracting the respective control. The PLP insensitive

radioactivity associated to the control samples was always less than 15% with respect to the PLP-sensitive TEA or acetylcholine transport. Data from dose response experiments, on WT and Cys mutants, were fitted with IC_{50} equation. Percentage residual activities with respect to the control are reported.

Other methods. The milligrams of reconstituted protein was estimated from Coomassie blue stained SDS-PAGE gels by using the Chemidoc imaging system equipped with Quantity One software (Bio-Rad) as previously described (Giancaspero *et al.*, 2013).

RESULTS

Effect of SH Reagents on TEA Transport

The effect of mercury compounds or Cd^{2+} has been tested on hOCTN1. As shown in Figure 1, the addition of $MeHg^{+}$ (as MeHgCl), Hg^{2+} (as $HgCl_2$), or Cd^{2+} ($CdCl_2$) caused strong inhibition of transport. The effect of DTE and natural scavengers in reversing the inhibition by mercury reagents was tested. As shown in Figure 1, DTE, Cys, and NAC reversed the inhibition by $MeHg^{+}$ and Hg^{2+} whereas their effect on Cd^{2+} was much less pronounced with the exception of DTE. S-carboxy-methyl-cysteine (CMC) did not exert any effect on the inhibition except that in the case of $MeHg^{+}$ in which 75% of the full activity was recovered.

The effect of chemical reagents which are known to form mixed disulfides with protein SH residues has also been tested. Among MTS compounds (MTSEA, MTSET, and MTSES), the most effective was MTSEA which exerted inhibition of transport very similar to that observed for the mercury compounds (not shown). The data on MTSEA, which is a specific SH reagent, indicated the possible of Cys residues of the protein in the inhibition.

To verify this hypothesis and to identify the target(s) of the reagents, Cys mutants of hOCTN1 have been constructed: each of the 7 Cys residues was substituted by Ala. The activity of the mutants was tested to verify whether one or more Cys residues were critical for the transport function of hOCTN1. As shown in Figure 2, the mutations only slightly influenced the [^{14}C]TEA transport. The time courses of C50A and C236A were nearly coincident with that of WT. The mutants C81A and C113A showed a slight reduction of the transport activity, whereas for C136A, C270A, and C374A, a lower transport activity was measured being, however, at least 60% of the WT activity (Fig. 2). Therefore, it could be concluded that the mutations of single Cys residues did not cause inactivation of hOCTN1, that is, no of the Cys residues is essential for function. Then, the dose-response curves of the transporter for each inhibitor were studied (Fig. 3). Mercury compounds were used at concentrations below 1mM to not disturb the liposome integrity. The mercury reagents showed similar behaviors: both Hg^{2+} (Fig. 3A) and $MeHg^{+}$ (Fig. 3B) strongly inhibited the WT and the mutants C81A, C113A, C236A, C270A, and C374A. The experimental data well fitted the dose-response equation with nearly complete inactivation of the transport at concentrations of the compounds far below 1mM. Interestingly, a clear shift of the curves toward higher concentrations of the compounds was observed in the case of mutants C50A and C136A, indicating a decrease of affinity of these mutants for the mercury reagents. The shift was more pronounced for C50A than for C136A, indicating that C50 has probably higher binding affinity toward the reagents. The IC_{50} values derived from the dose-response curves are reported in Table 1. The lower affinity measured for the C50A and C136A mutants indicated that C50 and, at a lower extent, C136 are the Cys involved in the binding of the mercury compounds. For a final proof of the role of C50 and C136, the double mutant C50A/C136A was constructed. The activity of this mutant was comparable to that of WT (not shown), indicating that the absence of both Cys residues did not alter the protein transport function. The dose-response analysis on the double mutant C50A/C136A showed a strong impairment of inhibition by Hg^{2+} and $MeHg^{+}$ with very high or not detectable IC_{50} values (Table 1). These results definitively demonstrate that the 2 Cys residues are the main targets of the mercury compounds (Fig. 3). The same experiments were conducted using MTSEA, a prototype SH reagent; in this case, the inhibition was sensibly reduced in the mutants C50A and C136A (Fig. 4 and Table 1). A decrease of inhibition by MTSEA was also observed in the C81A

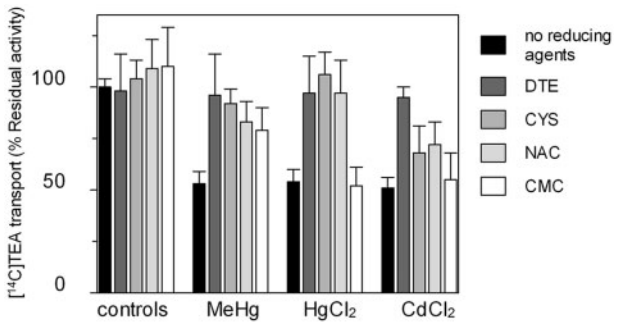

FIG. 1. Effect of DTE, Cys, NAC, and CMC on the inhibition of [^{14}C]TEA transport mediated by hOCTN1 reconstituted in liposomes in the absence and presence of mercuric reagents. 18μM $HgCl_2$ or MeHg, 46μM $CdCl_2$ and, after 10 min, 2.5 mM DTE or 5 mM Cys, NAC or CMC were added to proteoliposomes where indicated. After 10 min, proteoliposomes were passed through Sephadex G-75 columns and transport was started adding 0.1 mM [^{14}C]TEA and stopped after 30 min adding 3 mM PLP as described in Materials and Methods. Percent residual activity with respect to the control is reported. The values are means ± SD from 3 experiments.

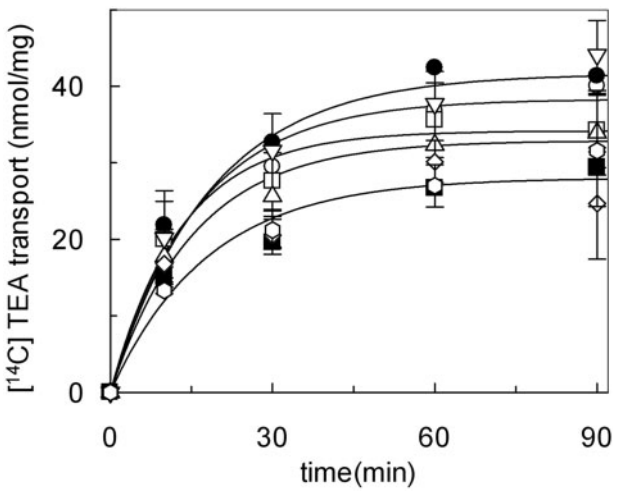

FIG. 2. Time courses of [^{14}C]TEA transport mediated by wild type and mutants of hOCTN1 reconstituted in liposomes. The reconstitution was performed as described in Materials and Methods. Transport was started by adding 0.1 mM [^{14}C]TEA at time zero to proteoliposomes reconstituted with WT (○), C50A (•), C81A (□), C113A (Δ), C136A (■), C236A (▽), C270A (◊), and C374A (). The curve of C50A is omitted because overlapping that of WT; the curves of C270A and C374A are omitted because overlapping that of C136A. The transport reaction was stopped at the indicated times adding 3 mM PLP and the specific transport activity (referred to as milligrams of proteins) was calculated according to the inhibitor-stop method as described in Materials and Methods. Results are means ± SD from 3 experiments.

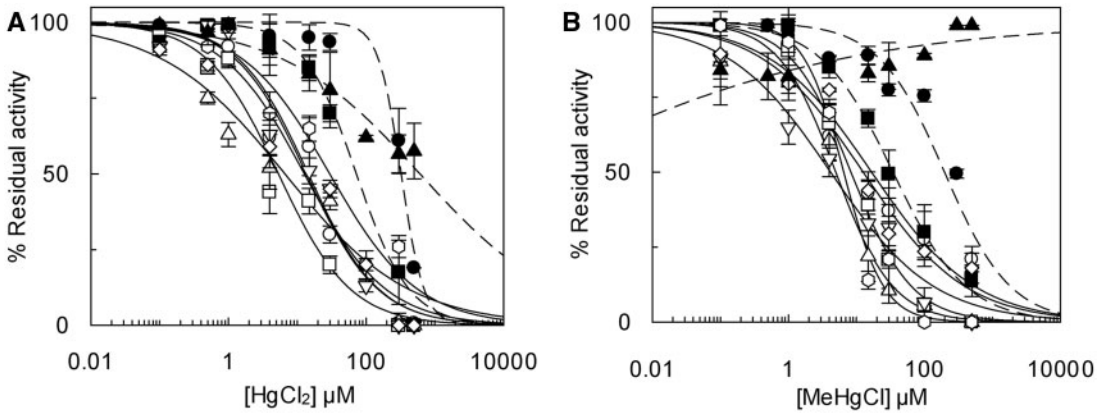

FIG. 3. Dose-response analysis of the inhibition of TEA transport by mercury compounds. Transport was measured in 10 min adding 0.1 mM [^{14}C]TEA to proteoliposomes reconstituted with hOCTN1 WT (○), C81A (□), C113A (Δ), C236A (▽), C270 (◊), C374A (), C50A (•), C136A (■), and C50A/C136A (▲). A, The indicated concentrations of $HgCl_2$ were added together with [^{14}C]TEA. B, The indicated concentrations of MeHgCl were added together with [^{14}C]TEA. Curves of mutants lacking inhibition are drown by dotted lines. Percent residual activity with respect to the control (in the absence of inhibitor) is reported. The values are means ± SD from 3 experiments.

TABLE 1. IC_{50} Values (µM) Calculated from Dose-Response Analysis for WT and 8 Mutant Proteins in the Presence of $HgCl_2$, MeHgCl, and MTSEA on [^{14}C]TEA Uptake

Protein	IC_{50} (µM)		
	$HgCl_2$	MeHgCl	MTSEA
WT	13.6 ± 2.7	16.8 ± 4.9	195.4 ± 43.7
C50A	324 ± 25**	198 ± 47*	756 ± 37*
C81A	5.3 ± 1.1	8.3 ± 1.3	458 ± 48
C113A	6.6 ± 3.3	5.0 ± 0.8	135 ± 18.6
C136A	72.7 ± 9.4**	34.6 ± 3.0	1411 ± 204*
C236A	14.5 ± 3.0	4.2 ± 1.0	91.2 ± 9.6
C270A	12.7 ± 4.3	12.6 ± 3.5	201 ± 28
C374A	29.7 ± 9.7	6.5 ± 1.0	164 ± 23
C50A/C136A	608 ± 159*	ND	1866 ± 106*

Notes: The values are means ± SD from 3 experiments. Significantly different from sample without added inhibitor as estimated by Student's *t* test (*$P < 0.005$; **$P < 0.001$).

mutant, even though less pronounced than in the mutants C50A and C136A. This indicated the possible involvement of an additional Cys residue in the reaction and inhibition by MTSEA. Accordingly, the double mutant C50A/C136A did not completely loose the sensitivity to MTSEA inhibition as in the case of the other reagents (Fig. 4). Indeed, even though the IC_{50} of the double mutant for MTSEA is higher than that for Hg^{2+}, this value is only one order of magnitude that of WT, whereas in the case of Hg^{2+}, the double mutant IC_{50} is 2 order of magnitudes that of WT. The data on MTSEA again confirmed the mechanism of inhibition, that is, reaction with SH groups of the protein.

Effect of SH Reagents on Acetylcholine Transport

The effect of the mercury reagents was tested also on transport of the physiological substrate acetylcholine. From the dose-response curves, it was evident that the mercury reagents behaved similarly as in the case of TEA transport (Fig. 5 and Table 2). Some of the IC_{50} for Hg^{2+} (Fig. 5A) and $MeHg^{+}$ (Fig. 5B) were slightly higher when measured with acetylcholine respect to TEA; in the case of the critical mutants C50A, C136A, and C50A/C136A, the experimental data could not be fitted in a dose-response equation (Fig. 5 and Table 2) except that in the case of the mutant C50A for Hg^{2+}, which anyway showed a considerable decrease of affinity.

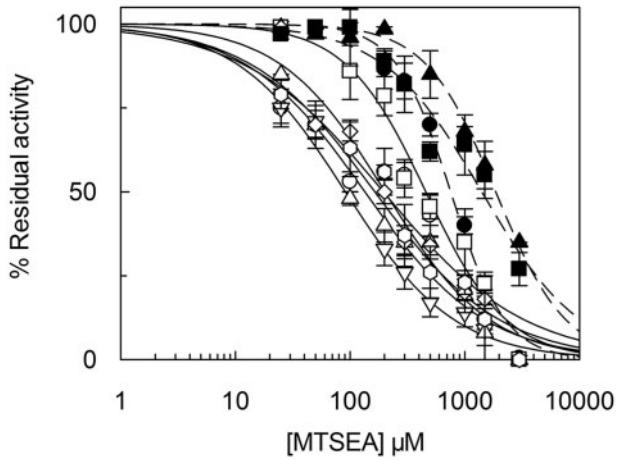

FIG. 4. Dose-response analysis of the inhibition of TEA transport by MTSEA. Transport was measured in 10 min adding 0.1 mM [^{14}C]TEA to proteoliposomes reconstituted with hOCTN1 WT (○), C81A (□), C113A (Δ), C236A (▽), C270 (◊), C374A (), C50A (•), C136A (■), and C50A/C136A (▲). The indicated concentrations of MTSEA were added together with [^{14}C]TEA. Curves of mutants lacking inhibition are drown by dotted lines. Percent residual activity with respect to the control (in the absence of inhibitor) is reported. The values are means ± SD from 3 experiments.

Effect of Ethyl Mercury on hOCTN1

$EtHg^{+}$ [used as $(C_2H_5HgS)C_6H_4CO_2Na$ (Thimerosal)] inhibited the hOCTN1 catalyzed transport as the other mercury compounds. Figure 6 shows the dose-response curves of WT and the critical mutants, that is, C50A, C136A, and C50A/C136A. The WT was potently inhibited by the reagent with an IC_{50} of 30µM both in the case of TEA (Fig. 6A) and acetylcholine (Fig. 6B) transport. The IC_{50} of the C50A for the reagent was much higher than that of WT, whereas the IC_{50} for C136A was only slightly higher than the WT. The data indicated that, in the case of $EtHg^{+}$, C50 is the main target of the reagent. The double mutant was nearly insensitive to $EtHg^{+}$ confirming the data on the single mutants. All the other mutants were inhibited with IC_{50} comparable to that of WT (not shown, but see Table 3).

Structural Model of hOCTN1

The homology model of hOCTN1 was built using as template the phosphate transporter PiPT (PDB 4J05) from the fungus

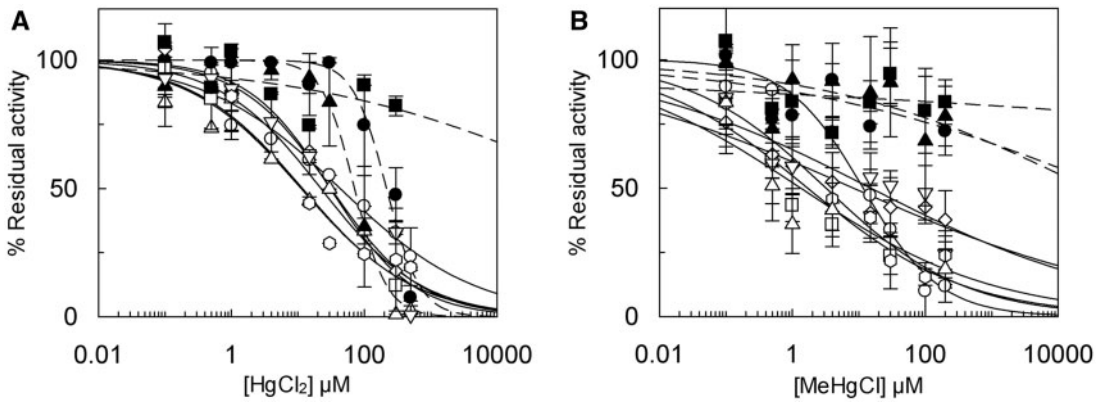

FIG. 5. Dose-response analysis of the inhibition of acetylcholine transport by mercury compounds. Transport was measured in 10 min adding 0.1 mM [^{3}H]Acetylcholine to proteoliposomes reconstituted with hOCTN1 WT (○), C81A (□), C113A (Δ), C236A (▽), C270 (◊), C374A (), C50A (•), C136A (■), and C50A/C136A (▲). A, The indicated concentrations of $HgCl_2$ were added together with [^{3}H]Acetylcholine. B, The indicated concentrations of MeHgCl were added together with [^{3}H]Acetylcholine. Curves of mutants lacking inhibition are drown by dotted lines. Percent residual activity with respect to the control (in the absence of inhibitor) is reported. The values are means ± SD from 3 experiments.

TABLE 2. IC_{50} Values (μM) Calculated from Dose-Response Curves for WT and 8 Mutant Proteins in the Presence of $HgCl_2$ and MeHgCl on [^{3}H]Acetylcholine Uptake

Protein	IC_{50} (μM)	
	$HgCl_2$	MeHgCl
WT	43.3 ± 9.6	11.6 ± 1.8
C50A	217 ± 28**	ND
C81A	22.2 ± 8.5	1.7 ± 0.9
C113A	11.2 ± 4.1	1.3 ± 1
C136A	ND	ND
C236A	31.4 ± 8.5	15 ± 10.7
C270A	30.7 ± 6.9	8.2 ± 2.6
C374A	11.7 ± 4.3	3.2 ± 1.2
C50A/C136A	ND	ND

Notes: The values are means ± SD from 3 experiments. Significantly different from sample without added inhibitor as estimated by Student's *t* test (**$P < 0.001$).

P. indica. As in previous cases, modeling of the large extracellular hydrophilic loop of hOCTN1 (Fig. 7A) was not possible. However, the identification of the Cys residues targeted by externally added mercury compounds allowed to validate some structural features. The hydrophilic loop (Fig. 7B) is exposed toward the extracellular surface even though its structure cannot be predicted with accuracy. The loss of inhibition by mercury compounds upon removal of C50, C136, and the impairment of inhibition by MTSEA after removal of C81 are in favor of the proposed localization of the loop. Moreover, the inhibition of the mutants C236A, C270A, and C374A at the same level of WT demonstrates that these residues are not involved in the inhibition. This confirms that these Cys residues are hidden and according to both the topology and structural models located in the transmembrane α-helices.

DISCUSSION

In the present work, structure/function relationships and molecular effects of mercury compounds on the human OCTN1 were investigated by using both experimental and computational approaches. According to the common mechanism of mercury action, that is, covalent binding to protein SH residues, evidences of interaction with Cys residues of hOCTN1 were provided: DTE and other SH reducing agents, such as Cys, specifically reverse S-X linkages, as previously demonstrated (Piermatti *et al.*, 2008; Pochini *et al.*, 2013a; Pochini *et al.*, 2009; Tonazzi *et al.*, 2013). In addition, the similar behavior of MTSEA, a specific SH reagent, further confirms the inhibition mechanism exerted by the toxic compounds on hOCTN1. Furthermore, computational analysis highlights the presence of 7 Cys residues in hOCTN1 primary structure, potentially involved in mercury interaction. Thus, by mean of site-directed mutagenesis, each of the 7 Cys residues has been substituted for Ala, normally used in Cys mutagenesis (Giangregorio *et al.*, 2013). The choice of Ala relies in the size and hydrophobicity of side chain, which are similar to those of Cys and in the inability to react with SH residues. The reconstitution in proteoliposomes of the single Cys mutants demonstrated that the major target of mercury compounds is C50; C136 can also react, even though at lower efficiency, with the smaller Hg^{2+} and $MeHg^{+}$. On the contrary, the reactivity of C136 with the larger $EtHg^{+}$ is very limited. This indicates that C136 is located in a smaller pocket and/or close to hydrophilic residues preventing the interaction with $EtHg^{+}$, which is also more hydrophobic than $MeHg^{+}$ and Hg^{2+}. The data were confirmed using a prototype SH reagent, MTSEA. Also in this case, the most critical residues were C50 together with C136. The very similar behavior with respect to the mercury compounds proved that the 2 Cys residues are critical for the described interaction. On the basis of the property of Hg^{2+}, it can be hypothesized that this reagent reacts with 2 SH groups forming a cross-link (van Iwaarden *et al.*, 1992). This is in line with the higher efficiency of interaction with both C50 and C136 with respect to $MeHg^{+}$, which is deduced by the higher IC_{50} measured upon the substitution of these residues (see Supplementary Information, Supplementary Table 1). The computational analysis revealed that all the reactive Cys are located in the extracellular loop of hOCTN1, being accessible to externally added reagents (Fig. 7A). Moreover, the hydrophilic nature of the extracellular loop promotes the reaction with the more hydrophilic compounds with respect to the hydrophobic ones. Indeed, the inhibition by MTSEA is reduced in the C81A mutant, indicating that also this Cys residue located at the beginning of the hydrophilic loop can be targeted by the reagent. But, neither

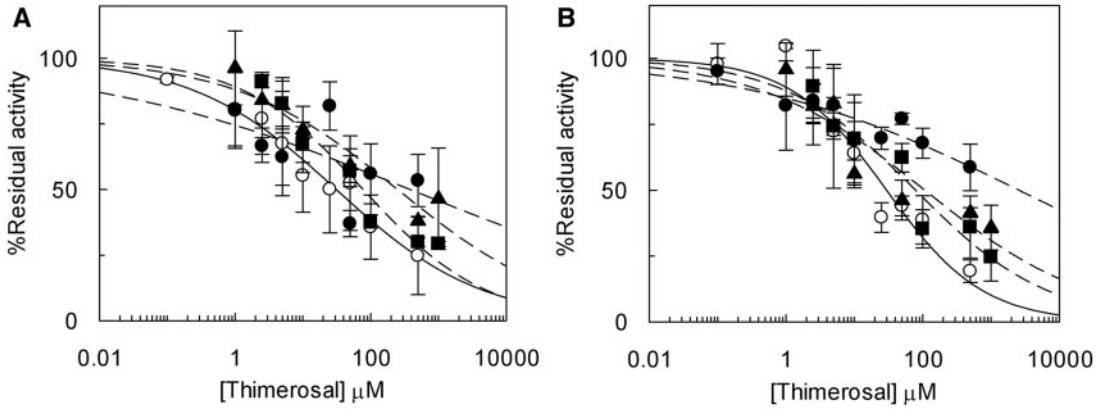

FIG. 6. Dose-response analysis of the inhibition by Thimerosal. Transport was measured in 10 min adding 0.1 mM [^{14}C]TEA (A) or [^{3}H]Acetylcholine (B) to proteoliposomes reconstituted with hOCTN1 WT (○),C50A (●), C136A (■), and C50A/C136A (▲). The indicated concentrations of Thimerosal ($EtHg^{+}$) were added together with [^{14}C]TEA (A) or [^{3}H]Acetylcholine (B). Curves of mutants lacking inhibition are drown by dotted lines. Percent residual activity with respect to the control (in the absence of inhibitor) is reported. The values are means ± SD from 3 experiments.

TABLE 3. IC_{50} Values (μM) Calculated from Dose-Response Curves for WT and 8 Mutant Proteins in the Presence of Thimerosal ($EtylHg^{+}$) on [^{14}C]TEA and [^{3}H]Acetylcholine Uptake

Protein	IC_{50} (μM) Thimerosal	
	[^{14}C]TEA	[^{3}H]Ach
WT	31 ± 5	30 ± 7
C50A	381 ± 90*	ND
C81A	40 ± 11	29 ± 14
C113A	21 ± 6.0	55 ± 12
C136A	78 ± 19	79 ± 23
C236A	32 ± 8.0	50 ± 12
C270A	55 ± 20	36 ± 13
C374A	46 ± 20	29 ± 6.2
C50A/C136A	107 ± 58	249 ± 93

Notes: The values are means ± SD from 3 experiments. Significantly different from sample without added inhibitor as estimated by Student's *t* test (*$P < 0.005$).

Hg^{2+} nor $MeHg^{+}$ lead to variation of effect on the C81A with respect to the WT, that is, this residue is not sensitive to Hg^{2+} and $MeHg^{+}$. This difference in reactivity can be explained in terms of steric hindrance. MTSEA, which is larger than mercurial reagents but more hydrophilic, binds to C81 and interferes with the transport pathway. At variance, the smaller mercury reagents do not bind or bind to without interfering with the transport pathway, for their smaller size with respect to MTSEA. Interestingly, some differences in the inhibition of the transporter and its mutants by MTSEA have been observed between the 2 substrates, TEA and acetylcholine. This accounts for a not complete overlap of the binding sites for the substrates. This has been previously hypothesized on the basis of the different structures of the cations as well as the behavior respect to their reciprocal inhibition (Pochini *et al.*, 2011, 2013b). Taken together, all the data obtained in this work are consistent with an orientation of hOCTN1 in proteoliposomes mimicking that of cell membrane. In this orientation, C50 and C136, as well as C81, are exposed toward the external environment thus being available to the reagents. Therefore, the data on inhibition allowed us to validate the homology model of the hOCTN1, reported in Figure 7B. Since C50, C81, and C136 can be targeted by mercurial reagents or MTSEA they cannot be involved in disulfides. The C113, even though is located in the extracellular loop, is not accessible to any of the mercury compound, since its mutation to Ala is ineffective and this mutant behaves as WT. According to their hidden intermembrane location, C236, C270, or C374 cannot be targeted, still validating the homology model proposed (Fig. 7B). Some of these residues may be involved in disulfides, as previously suggested on the basis of electrophoretic mobility of the same protein (Galluccio *et al.*, 2009). Further experiments are in the course for evaluating this hypothesis. The strength of the hOCTN1 model prediction also relies on the knowledge that phosphate transporter PiPT shares homology with the human SLC22 family members. In fact, homology models of OCT1 and OAT3 have been already obtained suggesting the suitability of PiPT structure for human homologs (Giacomini *et al.*, 2010; Pedersen *et al.*, 2013). hOCT1 was previously shown to be potently inhibited by mercury compounds (Pelis *et al.*, 2007). Interestingly, also in that case 2 major Cys residues were identified as targets of the mercury, which, on the basis of the homology model of hOCT1, lye in a hydrophilic cleft of the protein. So far, OCTs were recognized as drugs transporters; thus, impairment of their activity was thought to alter drug delivery or absorption (Giacomini *et al.*, 2010). The data described in this work shed new light on important physiopathological implication of hOCTN1. As previously reported, this transporter may be involved in control of inflammatory processes (Pochini *et al.*, 2012b). Being located in epithelial tissues, hOCTN1 can come in contact with toxic compound such as mercury compounds, cadmium, etc. when these are present at high concentration in the environment and/or in food. It has to be stressed that OCTN1 is expressed in intestine where the concentration of mercury compounds could reach concentrations higher than in plasma, following ingestion of contaminated food. Concentrations of mercury compounds of 0.15μM are reported in blood and other human tissues under normal conditions. These concentrations can increase up to 5μM due to exposure to pollutants (ATSDR 2007; Pochini *et al.*, 2013 and references herein), which are close to the IC_{50} value of hOCTN1 for mercury compounds. Measure of mercury compound concentrations in intestine is less reproducible than in other tissues. However, mercury in tuna fish has been found at concentration from about 0.2 up to 100μM depending on the low or high contamination degree (Schümann and Elsenhans, 2002). The highest concentration which could

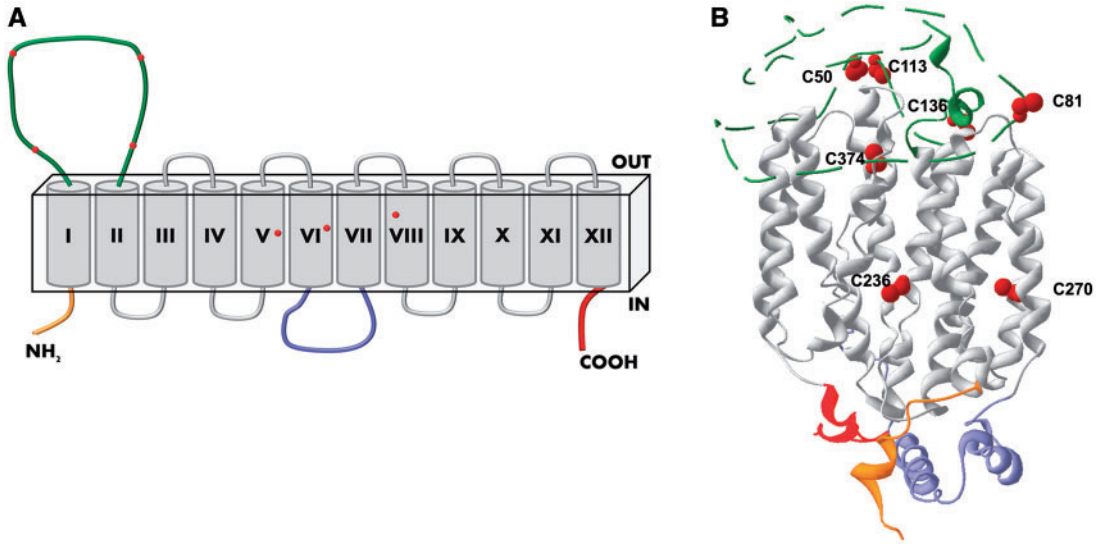

FIG. 7. Prediction of the hOCTN1 structure. A, Topology model obtained by hydropathy analysis of hOCTN1 protein using Kyte-Doolittle algorithm (window size = 21). Twelve membrane spanning domain are depicted as gray barrels. The 7 Cys residues are highlited as dots. The 2 large hydrophilic loops are depicted between membrane spanning domains I and II (extracellular) and and VI and VII (intracellular), respectively. N- and C-terminus face toward the intracellular side. B, Homology model of hOCTN1 protein. Ribbon representation of the hOTCN1 homology model. The structure was obtained from Phyre2 Server (Kelley and Sternberg, 2009) using the structure of eukaryotic phosphate transporter from *P. indica* (4J05) as template. 83% of the aa of the query are modeled at more than 90% accuracy. The large extracellular loop between the first and second transmembrane domain is not accurate and depicted as dotted coils. The side chains of the 7 Cys residues are highlited by numbered ball and sticks . The large loop between membrane spanning domains VI and VII, the N- and C-terminus protrude towards the intracellular side according to Figure 7A.

consequently be reached in intestine is much higher than the IC_{50} of hOCTN1 for mercury compounds (Pochini *et al.*, 2013a), which could easily interact with hOCTN1 causing inactivation of the transporter and, hence, impairment of acetylcholine release. Given that acetylcholine is involved in the control of inflammation in non-neuronal tissues, the impairment of the transporter will promote inflammatory processes, which may become chronic. This hypothesis correlates well with the recently reported inflammatory effects mediated by mercury compounds (Kempuraj *et al.*, 2010; Milnerowicz *et al.*, 2014).

An important contribute to toxicological aspect of hOCTN1 comes from the analysis of the inhibition by $EtHg^{+}$, which is still used as a preservative in some vaccines even though, in 2001, FDA removed it from childhood vaccines (http://www.fda.gov/BiologicsBloodVaccines/SafetyAvailability/VaccineSafety/UCM096228#t1, last accessed December 12, 2014) (Dorea *et al.*, 2013). Notwithstanding confusing and controversial information are present regarding $EtHg^{+}$ toxicity, we can assess that hOCTN1 is one of its targets and confirm that this compound interacts with Cys residues of proteins. Noteworthy, laboratory as well as pharmacological antioxidants reverse mercury inhibition. Some information has been reported also on Cd^{2+} interaction, which may have similar mechanism with respect to mercury compounds. This, however, needs further investigation. The reported data, together with the information on the mechanism of interaction with the transporter, have relevance on human health representing a potential intervention in mercury detoxification. Indeed, besides being effective on hOCTN1, the scavenger reagents NAC and Cys reverse mercury inhibition also in the case of other transporters potently inhibited by mercury compounds, that is, the carnitine transporter OCTN2 and the amino acid transporters ASCT2 and B0AT1 (Oppedisano *et al.*, 2010, 2011; Pochini *et al.*, 2013). Finally, the improved tridimensional structural model can give some efforts in drug design being hOCTN1 potential off-site target.

SUPPLEMENTARY DATA

Supplementary data are available online at http://toxsci.oxfordjournals.org/.

FUNDING

Ministry of Instruction University and Research (MIUR)-Italy, by a grant from PON-ricerca e competitività 2007-2013 (PON project 01_00937: "*Modelli sperimentali biotecnologici integrati per la produzione ed il monitoraggio di biomolecole di interesse per la salute dell'uomo*" to C.I.).

REFERENCES

ATSDR (Agency for Toxic Substrate and Disease Registry). (2007). *Toxicological Profile for Mercury*. U.S. Department of Health and Humans Services, Public Health Services, Center for Disease Control, Atlanta, GA.

Bridges, C. C., and Zalups, R. K. (2010). Transport of inorganic mercury and methylmercury in target tissues and organs. *J. Toxicol. Environ. Health. B. Crit. Rev.* **13,** 385–410.

Deng, D., Xu, C., Sun, P., Wu, J., Yan, C., Hu, M., and Yan, N. (2014). Crystal structure of the human glucose transporter GLUT1. *Nature* **510,** 121–125.

Dorea, J. G., Farina, M., and Rocha, J. B. (2013). Toxicity of ethylmercury (and Thimerosal): a comparison with methylmercury. *J. Appl. Toxicol.* **33,** 700–711.

Eraly, S. A., Monte, J. C., and Nigam, S. K. (2004). Novel slc22 transporter homologs in fly, worm, and human clarify the phylogeny of organic anion and cation transporters. *Physiol. Genomics* **18,** 12–24.

Galluccio, M., Pochini, L., Amelio, L., Accardi, R., Tommasino, M., and Indiveri, C. (2009). Over-expression in *E. coli* and purification of the human OCTN1 transport protein. *Protein. Expr. Purif.* **68,** 215–220.

Giacomini, K. M., Huang, S. M., Tweedie, D. J., Benet, L. Z., Brouwer, K. L., Chu, X., Dahlin, A., Evers, R., Fischer, V., Hillgren, K. M., *et al*. (2010). Membrane transporters in drug development. *Nat. Rev. Drug. Discov.* **9,** 215–236.

Giancaspero, T. A., Busco, G., Panebianco, C., Carmone, C., Miccolis, A., Liuzzi, G. M., Colella, M., and Barile, M. (2013). FAD synthesis and degradation in the nucleus create a local flavin cofactor pool. *J. Biol. Chem.* **288,** 29069–29080.

Giangregorio, N., Palmieri, F., and Indiveri, C. (2013). Glutathione controls the redox state of the mitochondrial carnitine/acylcarnitine carrier Cys residues by glutathionylation. *Biochim. Biophys. Acta* **1830,** 5299–5304.

Grundemann, D., Harlfinger, S., Golz, S., Geerts, A., Lazar, A., Berkels, R., Jung, N., Rubbert, A., and Schomig, E. (2005). Discovery of the ergothioneine transporter. *Proc. Natl Acad. Sci. U. S. A.* **102,** 5256–5261.

Ho, S. N., Hunt, H. D., Horton, R. M., Pullen, J. K., and Pease, L. R. (1989). Site-directed mutagenesis by overlap extension using the polymerase chain reaction. *Gene* **77,** 51–59.

Hopf, T. A., Colwell, L. J., Sheridan, R., Rost, B., Sander, C., and Marks, D. S. (2012). Three-dimensional structures of membrane proteins from genomic sequencing. *Cell* **149,** 1607–1621.

Huang, Y., Lemieux, M. J., Song, J., Auer, M., and Wang, D. N. (2003). Structure and mechanism of the glycerol-3-phosphate transporter from *Escherichia coli*. *Science* **301,** 616–620.

Indiveri, C., Galluccio, M., Scalise, M., and Pochini, L. (2013). Strategies of bacterial over expression of membrane transporters relevant in human health: the successful case of the three members of OCTN subfamily. *Mol. Biotechnol.* **54,** 724–36.

Indiveri, C., Palmieri, L., and Palmieri, F. (1994). Kinetic characterization of the reconstituted ornithine carrier from rat liver mitochondria. *Biochim. Biophys. Acta* **1188,** 293–301.

Indiveri, C., Pochini, L., Oppedisano, F., and Tonazzi, A. (2010). The carnitine transporter network: interactions with drugs. *Curr. Chem. Biol.* **4,** 108–123.

Indiveri, C., Tonazzi, A., Dierks, T., Kramer, R., and Palmieri, F. (1992). The mitochondrial carnitine carrier: characterization of SH-groups relevant for its transport function. *Biochim. Biophys. Acta* **1140,** 53–58.

Kato, Y., Kubo, Y., Iwata, D., Kato, S., Sudo, T., Sugiura, T., Kagaya, T., Wakayama, T., Hirayama, A., Sugimoto, M., *et al*. (2010). Gene knockout and metabolome analysis of carnitine/organic cation transporter OCTN1. *Pharm. Res.* **27**, 832–840.

Kelley, L. A., and Sternberg, M. J. (2009). Protein structure prediction on the Web: a case study using the Phyre server. *Nat. Protoc.* **4,** 363–371.

Kempuraj, D., Asadi, S., Zhang, B., Manola, A., Hogan, J., Peterson, E., and Theoharides, T. C. (2010). Mercury induces inflammatory mediator release from human mast cells. *J. Neuroinflammation* **7,** 20.

Lamhonwah, A. M., and Tein, I. (2006). Novel localization of OCTN1, an organic cation/carnitine transporter, to mammalian mitochondria. *Biophysics. Arch. Biochem. Biophys.* **345,** 1315–1325.

Milnerowicz, H., Sciskalska, M., and Dul, M. (2014). Pro-inflammatory effects of metals in persons and animals exposed to tobacco smoke. *J. Trace Elem. Med. Biol.* pii: S0946-672X(14)00064-9.

Nakamura, T., Yoshida, K., Yabuuchi, H., Maeda, T., and Tamai, I. (2008). Functional characterization of ergothioneine transport by rat organic cation/carnitine transporter Octn1 (slc22a4). *Biol. Pharm. Bull.* **31,** 1580–1584.

Oppedisano, F., Galluccio, M., and Indiveri, C. (2010). Inactivation by Hg2+ and methylmercury of the glutamine/amino acid transporter (ASCT2) reconstituted in liposomes: prediction of the involvement of a CXXC motif by homology modelling. *Biochem. Pharmacol.* **80,** 1266–1273.

Oppedisano, F., Pochini, L., Broer, S., and Indiveri, C. (2011). The B degrees AT1 amino acid transporter from rat kidney reconstituted in liposomes: kinetics and inactivation by methylmercury. *Biochim. Biophys. Acta* **1808,** 2551–2558.

Palmieri, F., and Klingenberg, M. (1979). Direct methods for measuring metabolite transport and distribution in mitochondria. *Methods Enzymol.* **56,** 279–301.

Pedersen, B. P., Kumar, H., Waight, A. B., Risenmay, A. J., Roe-Zurz, Z., Chau, B. H., Schlessinger, A., Bonomi, M., Harries, W., Sali, A., *et al*. (2013). Crystal structure of a eukaryotic phosphate transporter. *Nature* **496,** 533–536.

Pelis, R. M., Dangprapai, Y., Wunz, T. M., and Wright, S. H. (2007). Inorganic mercury interacts with cysteine residues (C451 and C474) of hOCT2 to reduce its transport activity. *Am. J. Physiol. Renal. Physiol.* **292,** F1583–F1591.

Peltekova, V. D., Wintle, R. F., Rubin, L. A., Amos, C. I., Huang, Q., Gu, X., Newman, B., Van Oene, M., Cescon, D., Greenberg, G., *et al*. (2004). Functional variants of OCTN cation transporter genes are associated with Crohn disease. *Nat. Genet.* **36,** 471–475.

Piermatti, O., Fringuelli, F., Pochini, L., Indiveri, C., and Palmerini, C. A. (2008). Synthesis and characterization of carnitine nitro-derivatives. *Bioorg. Med. Chem.* **16,** 1444–51.

Pochini, L., Peta, V., and Indiveri, C. (2013a). Inhibition of the OCTN2 carnitine transporter by $HgCl_2$ and methylmercury in the proteoliposome experimental model: insights in the mechanism of toxicity. *Toxicol. Mech. Methods* **23,** 68–76.

Pochini, L., Scalise, M., and Indiveri, C. (2009). Inactivation by omeprazole of the carnitine transporter (OCTN2) reconstituted in liposomes. *Chem. Biol. Interact.* **179,** 394–401.

Pochini, L., Scalise, M., Galluccio, M., Amelio, L., and Indiveri, C. (2011). Reconstitution in liposomes of the functionally active human OCTN1 (SLC22A4) transporter overexpressed in *Escherichia coli*. *Biochem. J.* **439,** 227–233.

Pochini, L., Scalise, M., Galluccio, M., and Indiveri, C. (2012a). Regulation by physiological cations of acetylcholine transport mediated by human OCTN1 (SLC22A4). Implications in the non-neuronal cholinergic system. *Life Sci.* **91,** 1013–1016.

Pochini, L., Scalise, M., Galluccio, M., and Indiveri, C. (2013b). OCTN cation transporters in health and disease: role as drug targets and assay development. *J. Biomol. Screen.* **18,** 851–67.

Pochini, L., Scalise, M., Galluccio, M., Pani, G., Siminovitch, K. A., and Indiveri, C. (2012b). The human OCTN1 (SLC22A4) reconstituted in liposomes catalyzes acetylcholine transport which is defective in the mutant L503F associated to the Crohn's disease. *Biochim. Biophys. Acta* **1818,** 559–565.

Pochini, L., Seidita, A., Sensi, C., Scalise, M., Eberini, I., and Indiveri C. (2014). Nimesulide binding site in the B0AT1 (SLC6A19) amino acid transporter. Mechanism of inhibition revealed by proteoliposome transport assay and molecular modelling. Biochem. Pharmacol. **89,** 422–430.

Rana, O. R., Schauerte, P., Kluttig, R., Schroder, J. W., Koenen, R. R., Weber, C., Nolte, K. W., Weis, J., Hoffmann, R., Marx, N., and Saygili, E. (2010). Acetylcholine as an age-

dependent non-neuronal source in the heart. *Auton. Neurosci.* **156,** 82–89.

Scalise, M., Galluccio, M., Pochini, L., and Indiveri, C. (2012). Overexpression in *Escherichia coli*, purification and reconstitution in liposomes of the third member of the OCTN sub-family: the mouse carnitine transporter OCTN3. *Biochem. Biophys. Res. Commun.* **422,** 59–63.

Scalise, M., Pochini, L., Giangregorio, N., Tonazzi, A., and Indiveri, C. (2013). Proteoliposomes as tool for assaying membrane transporter functions and interactions with xenobiotics. *Pharmaceutics* **5,** 472–497.

Schümann, K., and Elsenhans, B. (2002). The impact of food contaminants on the bioavailability of trace metals. J. Trace Elem. Med. Biol. **16,** 139–144.

Tamai, I., Ohashi, R., Nezu, J. I., Sai, Y., Kobayashi, D., Oku, A., Shimane, M., and Tsuji, A. (2000). Molecular and functional characterization of organic cation/carnitine transporter family in mice. *J. Biol. Chem.* **275,** 40064–40072.

Toh, D. S., Cheung, F. S., Murray, M., Pern, T. K., Lee, E. J., and Zhou, F. (2013). Functional analysis of novel variants in the organic cation/ergothioneine transporter 1 identified in Singapore populations. *Mol. Pharm.* **10,** 2509–2516.

Tonazzi, A., and Indiveri, C. (2011). Effects of heavy metal cations on the mitochondrial ornithine/citrulline transporter reconstituted in liposomes. *Biometals* **24,** 1205–1215.

Tonazzi, A., Eberini, I., and Indiveri, C. (2013). Molecular mechanism of inhibition of the mitochondrial carnitine/acylcarnitine transporter by omeprazole revealed by proteoliposome assay, mutagenesis and bioinformatics. *PLoS One* **8,** e82286.

van Iwaarden, P. R., Driessen, A. J., and Konings, W. N. (1992). What we can learn from the effects of thiol reagents on transport proteins. *Biochim. Biophys. Acta* **1113,** 161–170.

Wang, H., Yu, M., Ochani, M., Amella, C. A., Tanovic, M., Susarla, S., Li, J. H., Yang, H., Ulloa, L., Al-Abed, Y., *et al.* (2003). Nicotinic acetylcholine receptor alpha7 subunit is an essential regulator of inflammation. *Nature* **421,** 384–388.

Wessler, I., and Kirkpatrick, C. J. (2008). Acetylcholine beyond neurons: the non-neuronal cholinergic system in humans. *Br. J. Pharmacol.* **154,** 1558–1571.

Yabuuchi, H., Tamai, I., Nezu, J., Sakamoto, K., Oku, A., Shimane, M., Sai, Y., and Tsuji, A. (1999). Novel membrane transporter OCTN1 mediates multispecific, bidirectional, and pH-dependent transport of organic cations. *J. Pharmacol. Exp. Ther.* **289,** 768–773.

Yamashita, M., Yamashita, Y., Suzuki, T., Kani, Y., Mizusawa, N., Imamura, S., Takemoto, K., Hara, T., Hossain, M. A., Yabu, T., and Touhata, K. (2013). Selenoneine, a novel selenium-containing compound, mediates detoxification mechanisms against methylmercury accumulation and toxicity in zebrafish embryo. *Mar. Biotechnol. (NY)* **15,** 559–570.